Inorganic Chemistry

Article

pubs.acs.org/IC

Influencing the Size and Anion Selectivity of Dimeric Ln^{3+}[15-Metallacrown-5] Compartments through Systematic Variation of the Host Side Chains and Central Metal

Joseph Jankolovits, Choong-Sun Lim, Gellert Mezei, Jeff W. Kampf, and Vincent L. Pecoraro*

Department of Chemistry, University of Michigan, Ann Arbor, 930 North University Avenue, Ann Arbor, Michigan 48109, United States

Supporting Information

ABSTRACT: Dimeric Ln^{3+}[15-metallacrown-5] compartments selectively recognize carboxylates through guest binding to host metal ions and intermolecular interactions with the phenyl side chains. A systematic study is presented on how the size, selectivity, and number of encapsulated guests in the dimeric containers is influenced by the Ln^{3+}[15-metallacrown$_{Cu(II)}$-5] ligand side chain and central metal. Compartments of varying heights were assembled from metallacrowns with *S*-phenylglycine hydroxamic acid (pgHA), *S*-phenylalanine hydroxamic acid (pheHA), and *S*-homophenylalanine hydroxamic acid (hpheHA) ligands. Guests that were examined include the fully deprotonated forms of terephthalic acid, isonicotinic acid, and bithiophene dicarboxylic acid (btDC). X-ray crystallography reveals that the side-chain length constrains the maximum and minimum length guest that can be encapsulated in the compartment. Compartments with heights ranging from 9.7 to 15.2 Å are formed with different phenyl side chains that complex 4.3−9.2 Å long guests. Up to five guests are accommodated in Ln^{3+}[15-metallacrown$_{Cu(II)}$-5] compartments depending on steric effects from the host side chains. The nine-coordinate La^{3+} central metal promotes the encapsulation of multiple guests, while the eight-coordinate Gd^{3+} typically binds only one dicarboxylate. Electrospray ionization mass spectrometry reveals that the dimerization phenomenon occurs beyond the solid state, suggesting that these containers can be utilized in solid-state and solution applications.

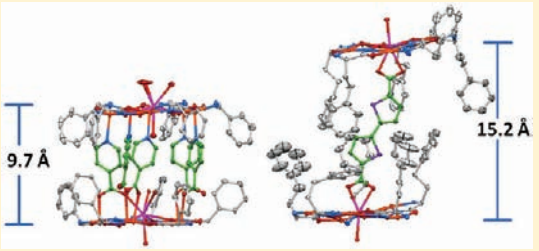

INTRODUCTION

Encapsulation of guests in molecular containers has implications for chemical transformations, sensing, stimuli-responsive devices, separations, and the design of molecular materials.[1−10] The expansive body of research on anion encapsulation focuses largely on organic hosts that recognize anions through noncovalent interactions such as hydrogen bonds and van der Waals forces. Molecular containers with open metal sites have drawn interest for the promise of novel guest selectivity, catalytic activity, and addressable properties that can arise from metal ions and concave cavities acting in concert.[11] Metalated container molecules display strong anion binding in aqueous solution due to strong electrostatic interactions between anions and the metal ions.[12−14] Furthermore, metal ions can impart spectroscopic, electrochemical, catalytic, magnetic, and structural properties to the host−guest complex not observed in traditional organic assemblies.[15−20] Rebek and co-workers prepared a Zn(II) metallocavitand that strongly binds phosphocholine esters[21] and catalyzes hydrolysis[22] and acetylation[23] reactions. Another benchmark example is Kersting's binuclear thiophenolate macrocyclic cavitand, which displays addressable magnetic and electrochemical properties.[24] Bound carboxylates undergo selective bromination[25] and Diels−Alder[26] reactions within the metallocavitand. Furthermore, the host forms dimeric capsules with bridging dicarboxylates.[27]

MCs are a unique class of self-assembled macrocycles with a metal-rich topology that resembles crown ethers.[28,29] These molecules formed some of the first molecular triangles,[30,31] squares,[32−34] and pentagons.[35−37] Many MCs selectively recognize anions through their open metal sites,[38−40] suggesting that novel molecular recognition chemistry could arise from embedding the MC in hydrophobic cavity. Ln^{3+}[15-$MC_{Cu(II)}$-5] complexes[41] (Scheme 1a) have been developed into chiral metallocavitands through synthesis with chiral *α*-amino hydroxamic acid ligands bearing hydrophobic side chains, such as *S*-phenylalanine hydroxamic acid (*S*-pheHA, Scheme 1c).[42] These metallocavitands display remarkable solution stability and bind anions to the Ln^{3+} central metal or Cu^{2+} ring metals.[43−45] The Ln^{3+}[15-$MC_{Cu(II)}$-5] hydrophobic cavity selectively recognizes carboxylate guests through hydrophobic interactions with the phenyl side chains.[46−48] Gd^{3+}[15-$MC_{Cu(II),\ S\text{-}pheHA}$-5]$^{3+}$ containers display enantioselectivity for particular *α*-amino acid analogs and show a strong thermodynamic preference for *α*-hydroxy-substituted carboxylates.[49] One promising application of Ln^{3+}[15-$MC_{Cu(II)}$-5] cavitands is using guest binding to prepare soft, chiral solids with functional topologies or addressable properties. In this regard, Ln^{3+}[15-$MC_{Cu(II)}$-5] complexes have been realized as resolved helices,[50]

Received: October 30, 2011
Published: February 6, 2012

dx.doi.org/10.1021/ic202347j | *Inorg. Chem.* 2012, 51, 4527−4538

Scheme 1. ChemDraw Diagrams of (a) Ln^{3+}[15-$MC_{Cu(II),\ S\text{-}\alpha\text{-}aminoHA}$-5], (b) *S*-pgHA, (c) *S*-pheHA, (d) *S*-hpheHA, (e) Isonicotinate, (f) Terephthalate, and (g) btDC[a]

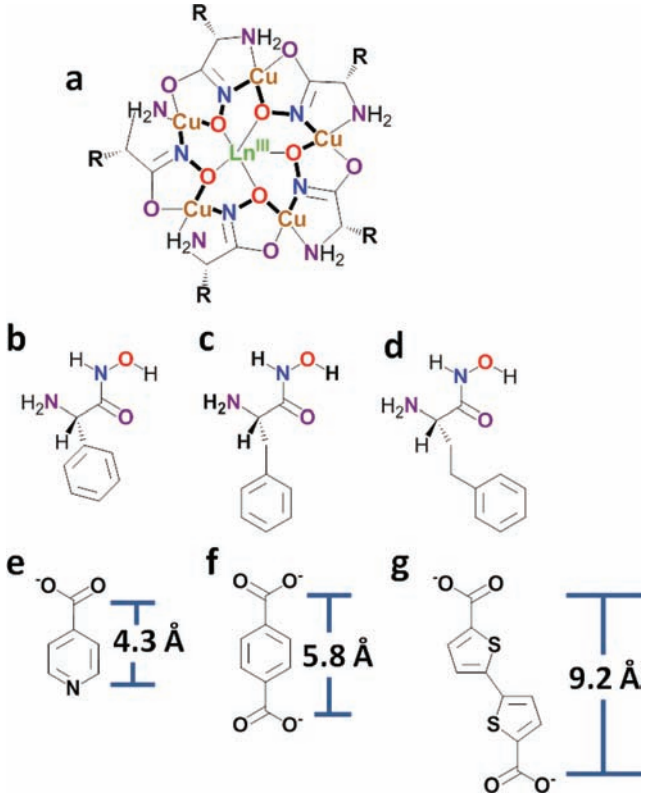

[a]The length of e corresponds to the pyridyl nitrogen to carboxylate carbon distance, while f and g are the carboxylate carbon to carboxylate carbon distances, as determined from crystal structures.

mesostructured assemblies,[51] dipolar solids displaying second-harmonic generation,[52] and dimeric molecular containers.[53] In addition, the Dy^{3+} analogue is a single-molecule magnet.[54] The supramolecular and chemical versatility of Ln^{3+}[15-$MC_{Cu(II)}$-5] complexes in solution and the solid state has prompted thorough studies of their guest recognition behavior that would aid in the application of these metallocavitands for a variety of applications, including catalysis, stimuli-responsive devices, and solid-state materials.

Dimeric compartments have been a consistent feature of Ln^{3+}[15-$MC_{Cu(II)}$-5] complexes in the solid state. These dimeric compartments assemble through supramolecular interactions between the Ln^{3+}[15-$MC_{Cu(II)}$-5] side chains. With *S*-tyrosine hydroxamic acid (tyrHA) ligands, the Ln^{3+}[15-$MC_{Cu(II),\ tyrHA}$-5] complexes dimerize through coordination of the phenol to a copper ring metal, resulting in a 7.6 Å tall cylindrical compartment that selectively encapsulates nitrate anions.[55] *S*-pheHA side chains associate through hydrophobic interactions, generating a larger dimeric compartment that encapsulates unsaturated dicarboxylate guests such as terephthalate (Figure 1f). These compartments show guest selectivity in the solid state, as all saturated dicarboxylates with a carbon chain length up to six have been excluded from the host's hydrophobic face.[42,56]

Previous characterization of Ln^{3+}[15-$MC_{Cu(II),\ pheHA}$-5] compartments reveals that the height of the compartment is guest dependent. The shortest compartment was the 10.3 Å tall Gd^{3+}[15-$MC_{Cu(II),\ pheHA}$-5](isonicotinate) complex.[52] The longest is the 12.1 Å Gd^{3+}[15-$MC_{Cu(II),\ pheHA}$-5](muconate) compartment.[56] Despite the differences in height, both compartments display π-stacking interactions between phenyl side chains that contribute to the integrity of the dimeric container. Notably, the maximum height of the Ln^{3+}[15-$MC_{Cu(II),\ pheHA}$-5] compartment is limited. Naphthalene dicarboxylate and bithiophene dicarboxylate (btDC) (guest lengths = 8.00 and 9.24 Å, respectively) disrupt compartment formation by preventing formation of associative π-stacking interactions between the two MCs.[56,57] Inclusion of multiple guests in Ln^{3+}[15-$MC_{Cu(II)}$-5] hosts has been observed in both monomeric MC complexes[46] and dimeric compartments.[52,55] Monomeric La^{3+}[15-$MC_{Cu(II)}$-5] complexes often bind two carboxylates in the hydrophobic cavity, which is afforded by the additional coordination site on the 9-coordinate La^{3+} central metal.[58] Gd^{3+}[15-$MC_{Cu(II)}$-5] hosts typically bind only one carboxylate guest that coordinates bidentate to the Gd^{3+} ion.

Given these observations in Ln^{3+}[15-$MC_{Cu(II),\ pheHA}$-5] compartments we sought to establish a theoretical framework for considering how the side-chain length influences the compartment size and number of encapsulated guests in dimeric Ln^{3+}[15-MC-5] containers. We hypothesized that the constraints on compartment height originate from the length of the phenyl side chain. Considering that the Ln^{3+}[15-$MC_{Cu(II),\ pheHA}$-5] compartment encapsulates terephthalate, we suspected that an MC with a shorter side chain would be incapable of forming a compartment with the 5.8 Å long guest. Following similar reasoning, we expected that a MC with a longer side chain would effectively encapsulate long guests that disrupt the Ln^{3+}[15-$MC_{Cu(II),\ pheHA}$-5] compartment. Lastly, we predicted that the side chain would limit the extent that a compartment can compress to encapsulate a short guest. Concerning inclusion of multiple guests in the compartments, we suspected that the nine-coordinate La^{3+} central metal would promote the inclusion of two guests based on the precedent in monomeric Ln^{3+}[15-$MC_{Cu(II),\ pheHA}$-5] complexes. Furthermore, we hypothesized that steric effects from the phenyl side chain would influence the number of encapsulated guests.

To address these issues of compartment size and selectivity, a series of Ln^{3+}[15-$MC_{Cu(II)}$-5] complexes has been synthesized from ligands bearing phenyl side chains that differ in the number of methylene carbons: *S*-phenylglycineHA (pgHA), *S*-pheHA, and *S*-homopheHA (hpheHA) (Scheme 1b, 1c, and 1d, respectively). The size and selectivity of this series of dimeric containers were assessed by examining the crystal structures of their inclusion complexes with a set of bridging guests that serve as molecular rulers: isonicotinate, terephthalate, and btDC (Scheme 1e, 1f, and 1g, respectively). Ln^{3+}[15-$MC_{Cu(II)}$-5] hosts with the 9-coordinate La^{3+} and 8-coordinate Gd^{3+} central metals have been employed to consider how the central metal coordination number influences the selectivity of the compartments. This work builds off of previous studies to establish a theoretical framework for predicting the structure of compartment inclusion complexes. The results presented herein reveal that the phenyl side chain dictates the maximum and minimum guest length that can be encapsulated in the compartment. The work also shows that steric effects from the side chain and the central metal coordination number can lead to the inclusion of up to five carboxylate guests in the compartments.

dx.doi.org/10.1021/ic202347j | *Inorg. Chem.* 2012, 51, 4527–4538

EXPERIMENTAL SECTION

All reagents were obtained from commercial sources and used as received unless specified. CHN analysis was performed by Atlantic Microlabs Inc. Bithiophene dicarboxylic acid was synthesized as previously described.[59] Sodium salts of isonicotinate and bithiophene dicarboxylic acid were prepared by neutralizing the respective carboxylic acid with sodium hydroxide in a water/methanol solution and precipitating with ether. The isolated solid was rinsed with ether and air dried. ESI-MS was performed with a Micromass LCT time-of-flight electrospray mass spectrometer at cone voltages ranging from 10 to 75 V on samples containing ~1 mg of compound dissolved in 1 mL of 4:1 methanol/water (v/v). Samples were injected via syringe pump. ESI-MS data was processed with MassLynx 4.0 software. Crystal structure images were prepared with Mercury 2.2.

Ligand Syntheses. Hydroxamic acid ligands were synthesized from the hydrochloric acid salts of their corresponding methyl esters following a modification of previously reported general procedures.[60] The procedure is outlined below for *S*-phenylglycine hydroxamic acid. The esters were obtained by refluxing a solution of the carboxylic acid and 1.5 equiv of thionyl chloride in dry methanol for 3 h followed by removal of the solvent under vacuum.

***S*-Phenylglycine Hydroxamic Acid.** Potassium hydroxide (0.045 mol, 2.88 g) was dissolved in 75 mL of degassed methanol and added to (*S*)-(+)-2-phenylglycine methyl ester hydrochloride (0.045 mol, 9.0 g). White potassium chloride quickly precipitated and was filtered after 10 min of cooling in an ice bath. Separately, hydroxylamine hydrochloride (0.134 mol, 9.30 g) was dissolved in 150 mL of degassed methanol, and another sample of potassium hydroxide (0.134 mol, 8.6 g) was dissolved in 125 mL of degassed methanol. The two solutions were combined and cooled in an ice bath under a stream of nitrogen to generate hydroxylamine and precipitate potassium chloride. The precipitate was filtered off, and the two filtrates were combined and stirred in a nitrogen atmosphere at room temperature. After 1 day, the hydroxamic acid precipitated as a white powder and was filtered. The filtrate was subjected to another portion of hydroxylamine and stirred overnight under nitrogen, and the hydroxamic acid precipitate was filtered. This filtrate was reduced to a volume of 40 mL under vacuum and allowed to sit for 4 days. Additional hydroxamic acid was isolated by filtration. The filtered solids were combined, stirred in 100 mL of water for 2 h as a fine suspension, and filtered. The solid was then stirred in 100 mL of dichloromethane for 1 h as a fine suspension and filtered. The solid was washed with ether and vacuum dried. Yield: 5.86 g (71%). ^{1}H NMR [$(CD_3)_2SO$, 400 MHz]: δ 8.8 (br s, 1H, NH) 7.35 (d, J = 7 Hz, 2H, *o*-Ph), 7.31 (t, J = 7 Hz, 2H, *m*-Ph), 7.22(t, J = 7 Hz, 1H, *p*-Ph), 4.22 (s, 1H, C_αH). MP = 172 °C. IR (KBr, cm^{-1}): 3032 br (NH, NH2, OH), 2878 br (CH), 2646 s (CH), 1612 s (C═O), 1542 m, 1467 m, 1362 m, 1312 w, 1276 w, 1199 w, 1017 w, 922 m, 819w, 776 w, 716 w, 693 m, 609 w. CHN found (calcd) for $C_8H_{10}N_2O_2$: C, 58.11 (57.82); H, 6.17 (6.07); N, 16.75(16.86).

S-Phenylalanine Hydroxamic Acid. Reaction was run on a 0.08 mol *S*-phenylalanine methyl ester hydrochloride scale. Yield: 12.19 g (85%). ^{1}H NMR [$(CD_3)_2SO$, 400 MHz]: δ 7.23 (m, 5H, Ph), 3.25 (t, J = 7 Hz, 1H, C_αH), 2.84 (q, J_1 = 13 Hz, J_2 = 6 Hz, 1H, C_βH), 2.61 (q, J_1 = 14 Hz, J_2 = 8 Hz, 1H, C_βH). MP = 190 °C. IR (KBr, cm^{-1}): 3028 br (NH, NH_2, OH), 2857 br (CH), 1615 s (C═O), 1557 m, 1534 m, 1466 m, 1383 s, 1288 s, 1174 w, 1072 w, 913 m, 886 m, 698 m. CHN found (calcd) for $C_9H_{12}N_2O_2$: C, 60.14 (59.97); H, 6.77 (6.71); N, 15.50(15.55).

S-Homophenylalanine Hydroxamic Acid. Reaction was run on a 0.075 mol (*S*)-homophenylalanine methyl ester hydrochloride scale. Yield: 12.61 g (87%). ^{1}H NMR [$(CD_3)_2SO$, 400 MHz]: δ 7.27 (t, J = 7 Hz, 2H, *m*-Ph), 7.17 (m, 3H, *o*-Ph, *m*-Ph) 3.02 (t, J = 7 Hz, 1H, C_αH), 2.62 (m, 1H, C_γH), 2.54 (m, 1H, C_γH), 1.78 (m, 1H, C_βH), 1.63 (m, 1H, C_βH). MP = 177.5 °C. IR (KBr, cm^{-1}): 3029 br (NH, NH_2, OH), 2859 br (CH), 1614 s (C═O), 1543 m, 1468 m, 1454 m, 1365 s, 1315 w, 1059 w, 942 w, 876 w, 775 w, 744 w, 696 w. CHN found (calcd) for $C_{10}H_{14}N_2O_2$: C, 62.07 (61.84); H, 7.41 (7.27); N, 14.32 (14.42).

Metallacrown Syntheses. La^{3+}[15-$MC_{Cu(II),\ S\text{-}pheHA}$-5]($NO_3$) and Gd^{3+}[15-$MC_{Cu(II),\ S\text{-}pheHA}$-5]($NO_3$) were prepared as previously described.[58]

La^{3+}[15-$MC_{Cu(II),\ S\text{-}pgHA}$-5]($NO_3$). *S*-phenylglycine hydroxamic acid (5 mmol, 0.83 g), copper acetate monohydrate (5 mmol, 1.00 g), and lanthanum nitrate hexahydrate (1 mmol, 0.43 g) were stirred overnight in 60 mL of methanol. The solution was filtered through a 2.5 cm shortpad of basic alumina (Brockman 1, Sigma-Aldrich) and rinsed through with 10 mL of methanol. The filtrate was dried under vacuum, yielding a dark purple solid. Yield: 1.293 g, 89%. ESI-MS: m/z 668.8^{2+} (668.9^{2+} calcd for [La^{3+}[15-$MC_{Cu(II),\ pgHA}$-5](NO_3^-)]$^{2+}$), 1399.8$^+$ (1398.8$^+$ calcd for [La^{3+}[15-$MC_{Cu(II),\ pgHA}$-5](NO_3^-)$_2$]$^+$). CHN found (calcd) for $LaCu_5C_{40}H_{40}N_{10}O_{10}(NO_3)_{1.5}(OH)_{1.5}(H_2O)_{3.5}$: C, 32.93 (32.96); H, 3.35 (3.24); N, 11.04 (11.04).

Gd^{3+}[15-$MC_{Cu(II),\ S\text{-}pgHA}$-5]($NO_3$). This compound was synthesized via the procedure for La^{3+}[15-$MC_{Cu(II),\ pgHA}$-5](NO_3), substituting gadolinium nitrate hexahydrate for lanthanum nitrate hexahydrate. Yield: 0.8213 g, 89%. ESI-MS: m/z 676.9^{2+} (678.4^{2+} calcd for [Gd^{3+}[15-$MC_{Cu(II),\ pgHA}$-5](NO_3^-)]$^{2+}$), 1418.8$^+$ (1417.8$^+$ calcd for [Gd^{3+}[15-$MC_{Cu(II),\ pgHA}$-5](NO_3^-)$_2$]$^+$). CHN found (calcd) for $GdCu_5C_{40}H_{40}N_{10}O_{10}(NO_3)_{0.5}(OH)_{2.5}(H_2O)_{3.5}$: C, 33.43 (33.54); H, 3.32 (3.48); N, 10.27 (10.30).

La^{3+}[15-$MC_{Cu(II),\ S\text{-}hpheHA}$-5]($NO_3$). This compound was synthesized via the procedure for La^{3+}[15-$MC_{Cu(II),\ pgHA}$-5](NO_3), substituting *S*-homopheHA for *S*-phenylglycineHA. Yield: 1.3899 g, 87%. ESI-MS: m/z 738.9^{2+} (740.0^{2+} calcd for [La^{3+}[15-$MC_{Cu(II),\ hpheHA}$-5](NO_3^-)]$^{2+}$), 1540.0$^+$ (1541.0$^+$ calcd for [La^{3+}[15-$MC_{Cu(II),\ hpheHA}$-5](NO_3^-)$_2$]$^+$). CHN found (calcd) for $LaCu_5C_{50}H_{60}N_{10}O_{10}(NO_3)_{1.5}(OH)_{1.5}(H_2O)_{3.5}$: C, 37.49 (37.55); H, 4.11 (4.32); N, 10.11 (10.07).

Gd^{3+}[15-$MC_{Cu(II),\ S\text{-}hpheHA}$-5]($NO_3$). This compound was synthesized via the procedure for La^{3+}[15-$MC_{Cu(II),\ hpheHA}$-5](NO_3), substituting gadolinium nitrate hexahydrate for lanthanum nitrate hexahydrate. Yield: 1.4726 g, 92%. ESI-MS: m/z 746.9^{2+} (748.5^{2+} calcd for [Gd^{3+}[15-$MC_{Cu(II),\ hpheHA}$-5](NO_3^-)]$^{2+}$), 1558.1$^+$ (1558.0$^+$ calcd for [Gd^{3+}[15-$MC_{Cu(II),\ hpheHA}$-5](NO_3^-)$_2$]$^+$). CHN found (calcd) for $GdCu_5C_{50}H_{60}N_{10}O_{10}(NO_3)(OH)_2(H_2O)_4$: C, 37.44 (37.44); H, 4.07 (4.44); N, 9.63 (9.66).

Synthesis of Host–Guest Complexes. Gd^{3+}[15-$MC_{Cu(II),\ S\text{-}pheHA}$-5](terephthalate)[42] and Gd^{3+}[15-$MC_{Cu(II),\ S\text{-}pheHA}$-5](isonicotinate)[52] were synthesized as previously described.

La^{3+}[15-$MC_{Cu(II),\ S\text{-}pgHA}$-5](isonicotinate). La^{3+}[15-$MC_{Cu(II),\ pgHA}$-5](NO_3) (0.021 mmol, 30 mg) and sodium isonicotinate (0.069 mmol, 10 mg) were dissolved in 5 mL of a 2:1 methanol/water mixture and filtered. Slow evaporation of the solvent yielded crystals within 1 month. Yield: 9.1 mg, 24%. ESI-MS: m/z 698.8^{2+} (698.9^{2+} calcd for {La^{3+}[15-$MC_{Cu(II),\ pgHA}$-5](isonicotinate$^-$)}$^{2+}$), 973.2^{3+} (973.3^{3+} calcd for {(La^{3+}[15-$MC_{Cu(II),\ pgHA}$-5])$_2$(isonicotinate$^-$)$_3$}$^{3+}$), 1521.9$^+$ (1520.9$^+$ calcd for {La^{3+}[15-$MC_{Cu(II),\ pgHA}$-5](isonicotinate$^-$)$_2$}$^+$). CHN found (calcd for $LaCu_5C_{40}H_{40}N_{10}O_{10}(C_6H_4NO_2)_{2.5}(OH)_{0.5}(H_2O)_{4.5}$): C, 39.32 (39.50); H, 3.38 (3.59); N, 10.33 (10.47).

La^{3+}[15-$MC_{Cu(II),\ S\text{-}pheHA}$-5](isonicotinate). La^{3+}[15-$MC_{Cu(II),\ pheHA}$-5](NO_3) (0.018 mmol, 30 mg) and sodium isonicotinate (0.069 mmol, 10 mg) were mixed in 6 mL of a 2:1 methanol/water mixture. The solution was filtered, and crystals were obtained within 2 months upon slow evaporation of the solvent. Yield: 14.6 mg, 46%. ESI-MS: m/z 733.9^{2+} (735.0^{2+} calcd for{La^{3+}[15-$MC_{Cu(II),pheHA}$-5](isonicotinate$^-$)}$^{2+}$), 1019.9^{3+} (1020.0 calcd for {(La^{3+}[15-$MC_{Cu(II),\ pheHA}$-5])$_2$(isonicotinate$^-$)$_3$}$^{3+}$), 1590.0$^+$ (1591.0$^+$ calcd for{La^{3+}[15-$MC_{Cu(II),\ pheHA}$-5](isonicotinate$^-$)$_2$}$^+$). CHN found (calcd for $LaCu_5C_{45}H_{50}N_{10}O_{10}(C_6H_4NO_2)_2(NO_3)(H_2O)_6$): C, 38.74 (38.85); H, 3.98 (4.01); N = 10.08 (10.34).

La^{3+}[15-$MC_{Cu(II),\ hpheHA}$-5](isonicotinate). La^{3+}[15-$MC_{Cu(II),\ hpheHA}$-5](NO_3) (0.019 mmol, 30 mg) and sodium isonicotinate (0.069 mmol, 10 mg) were combined in 8 mL of a 3:1 methanol/water mixture. The solution was filtered and set to slowly evaporate. Crystals formed in 2 weeks. Yield: 9.8 mg, 29%. ESI-MS: m/z 768.9^{2+} (770.0^{2+} calcd for{La^{3+}[15-$MC_{Cu(II),\ hpheHA}$-5](isonicotinate$^-$)}$^{2+}$), 1066.7^{3+} (1067.4^{3+} calcd for {(La^{3+}[15-$MC_{Cu(II),\ hpheHA}$-5])$_2$(isonicotinate$^-$)$_3$}$^{3+}$), 1660.1$^+$ (1661.0$^+$ calcd for {La^{3+}[15-$MC_{Cu(II),\ hpheHA}$-5](isonicotinate$^-$)$_2$}$^+$). CHN found (calcd for

dx.doi.org/10.1021/ic202347j | Inorg. Chem. 2012, 51, 4527–4538

$LaCu_5C_{50}H_{60}N_{10}O_{10}(C_6H_4NO_2)_2(NO_3)(H_2O)_{3.5}$: C, 41.50 (41.67); H, 4.15 (4.23); N, 9.72 (10.19).

La^{3+}[15-$MC_{Cu(II),\ pheHA}$-5](terephthalate). La^{3+}[15-$MC_{Cu(II),\ pheHA}$-5](NO_3) (0.018 mmol, 30 mg) and terephthalic acid sodium salt (0.027 mmol, 5.7 mg) were dissolved in 8 mL of a 3:1 methanol/water mixture. The solution was set to slowly evaporate, yielding crystals within 1 month. Yield: 22.7 mg, 76%. ESI-MS: m/z 755.4^{2+} (756.5^{2+} calcd for $\{La^{3+}[15\text{-}MC_{Cu(II),\ pheHA}\text{-}5](terephthalateH^-)]\}^{2+}$), 973.3^{3+} (973.3^{3+} calcd for $\{(La^{3+}[15\text{-}MC_{Cu(II),\ pheHA}\text{-}5])_2(terephthalate^{2-})(NO_3^-)\}^{3+}$), 1007.6^{3+} (1007.6^{3+} calcd for $[La^{3+}[15\text{-}MC_{Cu(II),\ pheHA}\text{-}5](terephthalate^{2-})(terephthalateH^-)\}^{3+}$), 1511.0^{+} (1509.9^{+} calcd for $\{La^{3+}[15\text{-}MC_{Cu(II),\ pheHA}\text{-}5](terephthalate^{2-})\}^{+}$), 1511.0^{2+} (1511.0^{2+} calcd for $[(La^{3+}\{15\text{-}MC_{Cu(II),\ pheHA}\text{-}5])_2(terephthalate^{2-})_2\}^{2+}$). CHN found (calcd for $LaCu_5C_{45}H_{50}N_{10}O_{10}(C_8H_4O_4)(NO_3)(H_2O)_5$): C, 38.38 (38.26); H, 3.77 (3.88); N, 9.11 (9.26).

La^{3+}[15-$MC_{Cu(II),\ hpheHA}$-5](terephthalate). La^{3+}[15-$MC_{Cu(II),\ hpheHA}$-5](NO_3) (0.019 mmol, 30 mg) and terephthalic acid sodium salt (0.048 mmol, 10 mg) were mixed in 8 mL of a 3:1 methanol/water fixture and filtered. The solvent slowly evaporated, yielding crystals in two weeks. Yield: 16.3 mg, 49%. ESI-MS: m/z 790.5^{2+} (791.5^{2+}calcd for $\{La_3^{+}[15\text{-}MC_{Cu(II),\ hpheHA}\text{-}5](terephthalateH^-)\}^{2+}$), 1055.0^{3+} (1055.0^{3+} calcd for $\{(La^{3+}[15\text{-}MC_{Cu(II),\ hpheHA}\text{-}5])_2(terephthalate^{2-})(terephthalateH^-)\}^{3+}$), 1061.7^{3+} (1062.3 calcd for $\{(La^{3+}[15\text{-}MC_{Cu(II),\ hpheHA}\text{-}5])_2(terephthalate^{2-})(terephthalateH^-)(H_2O)\}^{3+}$), 1581.0^{+} (1581.6^{+} calcd for$\{La^{3+}[15\text{-}MC_{Cu(II),\ hpheHA}\text{-}5](terephthalate^{2-})\}^{+}$), 1581.0^{2+} (1581.6^{2+} calcd for $\{(La^{3+}[15\text{-}MC_{Cu(II),\ hpheHA}\text{-}5])_2(terephthalate^{2-})_2\}^{2+}$). CHN found (calcd for $LaCu_5C_{50}H_{60}N_{10}O_{10}(C_8H_4O_4)_{1.5}(H_2O)_5$): C, 42.36 (42.46); H, 4.17 (4.37); N, 7.95 (7.99).

Gd^{3+}[15-$MC_{Cu(II),\ pgHA}$-5](terephthalate). Gd^{3+}[15-$MC_{Cu(II),\ pgHA}$-5](NO_3) (0.021 mmol, 30 mg) was dissolved in 5 mL of water. Terephthalic acid sodium salt (0.06 mmol, 12.6 mg) was dissolved in about 2 mL of water. The solution was filtered, and crystals were obtained upon slow evaporation of the solvent. Yield: 3.4 mg, 8.7%. ESI-MS: m/z 729.9^{2+} (729.9^{2+} calcd for $\{Gd^{3+}[15\text{-}MC_{Cu(II),\ pgHA}\text{-}5](terephthalateH^-)\}^{2+}$), 972.8^{3+} (973.6^{3+} calcd for $\{Gd^{3+}[15\text{-}MC_{Cu(II),\ pgHA}\text{-}5](terephthalate^{2-})(terephthalateH^-)\}^{3+}$), 1460.0^{+} (1458.9^{+} calcd for $[Gd^{3+}[15\text{-}MC_{Cu(II),\ pgHA}\text{-}5](terephthalate^{2-})\}^{+}$, 1460.0^{2+} (1460.0^{2+} calcd for $[(Gd^{3+}[15\text{-}MC_{Cu(II),\ pgHA}\text{-}5])_2(terephthalate^{2-})_2\}^{2+}$), 1625.0^{+} (1624.9^{+} calcd for $\{Gd^{3+}[15\text{-}MC_{Cu(II),\ pgHA}\text{-}5](terephthalateH^-)_2\}^{+}$). CHN found (calcd for $GdCu_5C_{40}H_{40}N_{10}O_{10}(C_8H_4O_4)(C_8H_5O_4)(H_2O)_{13}$): C, 35.53 (36.18); H, 3.51 (4.07); N, 8.14 (7.53).

Gd^{3+}[15-$MC_{Cu(II),\ hpheHA}$-5](terephthalate). Gd^{3+}[15-$MC_{Cu(II),\ hpheHA}$-5](NO_3) (0.019 mmol, 30 mg) and terephthalic acid sodium salt (0.027 mmol, 5.7 mg) were dissolved in 10 mL of ethanol and 3 mL of water. The solution was filtered, and deep purple crystals were obtained upon slow evaporation of the solvent. Yield: 8.7 mg, 27%. ESI-MS: m/z 800.0^{2+} (800.0^{2+} calcd for $\{Gd^{3+}[15\text{-}MC_{Cu(II),\ hpheHA}\text{-}5](terephthalateH^-)\}^{2+}$), 1067.7^{3+} (1067.0^{3+} calcd for $\{(Gd^{3+}[15\text{-}MC_{Cu(II),\ hpheHA}\text{-}5])_2(terephthalate^{2-})(terephthalateH^-)\}^{3+}$), 1074.4^{3+} (1073.0^{3+} calcd for$\{(Gd^{3+}[15\text{-}MC_{Cu(II),\ hpheHA}\text{-}5])_2(terephthalate^{2-})(terephthalateH^-)(H_2O)\}^{3+}$, 1600.1^{+} (1600.0^{+} calcd for$\{Gd^{3+}[15\text{-}MC_{Cu(II),\ hpheHA}\text{-}5](terephthalate^{2-})\}^{+}$, 1600.1^{2+} (1600.0^{2+} calcd for$\{(Gd^{3+}[15\text{-}MC_{Cu(II),\ hpheHA}\text{-}5])_2(terephthalate^{2-})_2\}^{2+}$). CHN found (calcd for $GdCu_5C_{50}H_{60}N_{10}O_{10}(C_8H_4O_4)(OH)(C_2H_6O)_{0.5}(H_2O)_4$): C, 41.47 (41.39); H, 4.12 (4.47); N, 7.83 (8.18).

Gd^{3+}[15-$MC_{Cu(II),\ hpheHA}$-5](btDC). Gd^{3+}[15-$MC_{Cu(II),\ hpheHA}$-5](NO_3) (0.019 mmol, 30 mg) and 2,2′-bithiophene dicarboxylic acid disodium salt (0.027 mmol, 8.2 mg) were mixed in 6 mL of a 2:1 DMF/water mixture. The solution was filtered. Water (4 mL) was slowly added until the blue precipitate persisted. Methanol (1 mL) was added to clarify the solution, which was slowly evaporated to yield crystals in under 2 weeks. Yield: 13.5 mg, 37%. ESI-MS: m/z 843.9^{2+} (845.0^{2+} calcd for $\{Gd^{3+}[15\text{-}MC_{Cu(II),\ hpheHA}\text{-}5](btDCH^-)\}^{2+}$), 880.5^{2+} (881.5^{2+} calcd for $\{Gd^{3+}[15\text{-}MC_{Cu(II),\ hpheHA}\text{-}5](btDCH^-)(DMF)\}^{2+}$), 1125.6^{3+} (1125.7^{2+} calcd for $\{(Gd^{3+}[15\text{-}MC_{Cu(II),\ hpheHA}\text{-}5])_2(btDC^{2-})(btDCH^-)\}^{3+}$, 1688.0^{+} (1688.0^{+} calcd for $\{Gd^{3+}[15\text{-}MC_{Cu(II),\ hpheHA}\text{-}5](btDC^{2-})\}^{+}$), 1688.0^{2+} (1688.0^{2+} calcd for $\{(Gd^{3+}[15\text{-}MC_{Cu(II),\ hpheHA}\text{-}5])_2(btDC^{2-})_2\}^{+}$). CHN found (calcd for $GdCu_5C_{50}H_{60}N_{10}O_{10}(C_{10}H_4O_4S_2)_{1.5}(H_2O)_7$): C, 40.05 (40.23); H, 4.13 (4.16); N, 7.37 (7.22).

La^{3+}[15-$MC_{Cu(II),\ pgHA}$-5](btDC). La^{3+}[15-$MC_{Cu(II),\ pgHA}$-5](NO_3) (0.021 mmol, 30 mg) and 2,2′-bithiophene dicarboxylic acid disodium salt (0.034 mmol, 10 mg) were mixed in 12 mL of a 2:2:1 methanol/water/acetonitrile mixture. A blue precipitate formed and was redissolved upon the addition of 3 mL of DMF. The solution was filtered and set to slowly evaporate, yielding crystals in 1 month. Yield: 8.4 mg, 22%. ESI-MS: m/z 765.3^{2+} (765.4^{2+} calcd for $\{La^{3+}[15\text{-}MC_{Cu(II),\ pgHA}\text{-}5](btDCH^-)\}^{2+}$), 801.9^{2+} (801.9^{2+} calcd for $\{La^{3+}[15\text{-}MC_{Cu(II),\ pgHA}\text{-}5](btDCH^-)(DMF)\}^{2+}$), 1529.8^{+} (1528.8^{+} calcd for $\{La^{3+}[15\text{-}MC_{Cu(II),\ pgHA}\text{-}5](btDC^{2-})\}^{+}$), 1529.8^{2+} (1528.8^{2+} calcd for $\{(La^{3+}[15\text{-}MC_{Cu(II),\ pgHA}\text{-}5])_2(btDC^{2-})_2\}^{2+}$). CHN found (calcd for $LaCu_5C_{40}H_{40}N_{10}O_{10}(C_{10}H_4O_4S_2)_{1.5}(H_2O)_9$): C, 36.23 (36.34); H, 3.62 (3.55); N, 7.88 (7.70).

Crystallography. Intensity data for La^{3+}[15-$MC_{Cu(II),\ pgHA}$-5]-(btDC) was collected at 150 K on a D8 goniostat equipped with a Bruker APEXII CCD detector at Beamline 11.3.1 at the Advanced Light Source (Lawrence Berkeley National Laboratory) using synchrotron radiation tuned to λ = 0.7749 Å. A series of 3 s frames measured at 0.2° increments of ω were collected to calculate a unit cell. For data collection frames were measured for a duration of 3 s for low-angle data and 5 s for high-angle data at 0.3° intervals of ω with a maximum 2θ value of ~60°. Data frames were collected using APEX2 and processed using the program SAINT[61] routine within APEX2. Data were corrected for absorption and beam corrections based on the multiscan technique as implemented in SADABS.[62] The structure was solved and refined with the Bruker SHELXTL (version 2008/4) software package.[63]

Intensity data for La^{3+}[15-$MC_{Cu(II),\ pheHA}$-5](isonicotinate) was collected at 85(2) K on a standard Bruker SMART-APEX CCD-based X-ray diffractometer equipped with a low-temperature device and fine focus Mo-target X-ray tube (λ = 0.71073 A) operated at 1500 W power (50 kV, 30 mA). Indexing was performed by use of the CELL_NOW[64] program, which indicated that the crystal was a two-component, nonmerohedral twin. Analysis of the data showed negligible decay during data collection; data were processed with TWINABS[65] and corrected for absorption. The domains are related by a rotation of 2.3° about the reciprocal [0.660 1.000 0.274] axis or direct [0.505 1.000 −0.169] axis. For this refinement, single and composite reflections from the primary domain were used. Merging of the data was performed in TWINABS[65] and an HKLF 4 format file used for refinement. Structures were solved and refined with the Bruker SHELXTL (version 2008/4) software package.[63]

Intensity data for all other samples were collected at 85(2) K on a standard Bruker SMART-APEX CCD-based X-ray diffractometer equipped with a low-temperature device and fine focus Mo-target X-ray tube (λ = 0.71073 A) operated at 1500 W power (50 kV, 30 mA). Frames were integrated with the Bruker SAINT software package[61] with a narrow-frame algorithm. Data were processed with SADABS[62] and corrected for absorption. Structures were solved and refined with the Bruker SHELXTL (version 2008/4) software package.[63]

Additional crystallographic details are presented in Table 1. CIF files and crystallographic tables for all structures are presented in the Supporting Information.

RESULTS AND DISCUSSION

Compartments. In terms of their covalent structure, Ln^{3+}[15-$MC_{Cu(II),\ pheHA}$-5] complexes are monomeric metallocavitands. Crystal structures of the hosts with certain bridging carboxylate guests reveal dimeric compartments that form through associative hydrophobic interactions between phenyl rings on the ligand side chains. We recognized certain structural criteria for Ln^{3+}[15-$MC_{Cu(II),\ S\text{-}pheHA}$-5] compartments.[42,48,56] First, compartments contain hydrophobic interactions between phenyl side chains on adjacent LnMCs, effectively creating the walls of the container. Second, compartments typically possess

dx.doi.org/10.1021/ic202347j | Inorg. Chem. 2012, 51, 4527−4538

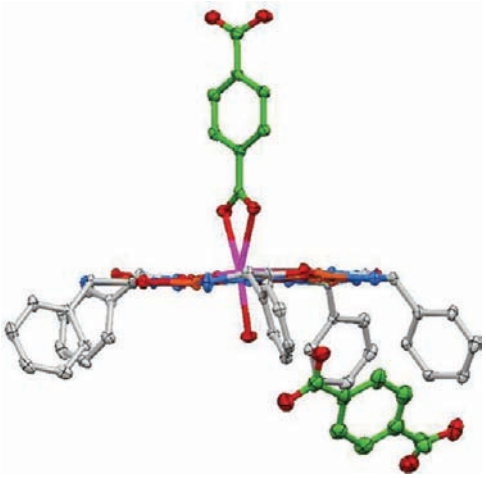

Figure 1. Thermal ellipsoid plot of Gd^{3+}[15-$MC_{Cu(II),\ pgHA}$-5]-(terephthalate). Color scheme: pink = Gd, orange = Cu, red = O, dark blue = N, gray = MC C, green = guest C. Lattice solvent molecules and hydrogen atoms were removed for clarity. Thermal ellipsoids are displayed with 50% probability.

an approximately cylindrical shape in order to maximize associative contacts between phenyl side chains and completely encapsulate the guest. Third, the Ln^{3+}[15-$MC_{Cu(II)}$-5] phenyl side chains recognize guests through directional, convergent intermolecular interactions. As a whole, these features define the compartment as a dimeric container that recognizes guests through both dative bonds and intermolecular interactions. The solid-state guest recognition described herein has straightforward implications for application of the Ln^{3+}[15-$MC_{Cu(II)}$-5] compartment as a crystalline molecular flask for solid-state reactions.[66] Importantly, the associative phenyl interactions between ligand side chains would contribute to compartment formation in the absence of solid-state packing forces, suggesting the possibility of solution applications for these hosts.

Compartment height is a significant characteristic of Ln^{3+}[15-$MC_{Cu(II)}$-5] dimers. In this work, we report compartment heights (or MC−MC distance) as the distance between the centroid of the oxygen-mean planes of each MC.[67] Given that the location of the central metal varies from approximately 0.2 to 0.7 Å above or below the center of the oxygen-mean plane,[58] referencing compartment dimensions to the center of the oxygen-mean plane allows for more direct comparisons of different structures. Given the dependence of the compartment's dimensions on guest size, we investigated guests of varying length in order to assess how side-chain variation effects compartment size and selectivity. Guest length is defined as the distance between carboxylate carbons for dicarboxylates or carboxylate carbon to pyridyl nitrogen for isonicotinate. Referencing guest length to the carboxylate carbon eliminates the disparity between endo and exo carboxylate binding. In the specific case of the btDC guest, the length can vary by over 0.3 Å depending on the torsion angle between the two thiophene rings. The trans rotamer distance is reported in Scheme 1.

Side-Chain Length Constrains the Compartment Height. It has previously been demonstrated that the 5.8 Å long terephthalate guest is effectively encapsulated in the dimeric Gd^{3+}[15-$MC_{Cu(II),\ pheHA}$-5] container.[42] It has also been shown that the maximum compartment height is constrained, as the compartment does not form with naphthalene dicarboxylate or btDC.[56,57] Complexes between the Ln^{3+}[15-$MC_{Cu(II),\ pgHA}$-5] host and terephthalate and btDC guests presented herein establish further that long guests lead to compartment disruption by associative intermetallacrown interactions between the phenyl side chains that are necessary for compartment integrity.

In the Gd^{3+}[15-$MC_{Cu(II),\ pgHA}$-5](terephthalate) complex (Figure 1) a monomeric host is observed with terephthalate-bound bidentate on the hydrophilic face. The other carboxylate on this terephthalate forms hydrogen bonds with lattice water molecules. On the hydrophobic face a water is bound to Gd^{3+}. An unbound terephthalate forms a hydrogen bond with this coordinated water and π-stacking interactions with pgHA phenyl rings. Unlike other MC structures, the saturated guest is not bound to the lanthanide central metal on the hydrophobic face. This is attributed to the orientation of the inflexible phenyl side chain toward the periphery of the MC, which limits how effectively the phenyl side chains can recognize a guest bound to the central metal. Importantly, this structure shows that the short pgHA side chain prevents compartment formation with the 5.8 Å long terephthalate. In contrast, a compartment is observed in the Ln^{3+}[15-$MC_{Cu(II),\ pheHA}$-5](terephthalate) complexes with La^{3+} (vide infra) and Gd^{3+}, which further demonstrates that the maximum allowed compartment height is constrained by side-chain length.

Unsurprisingly, the prototypical cylindrical compartment is also not observed in the La^{3+}[15-$MC_{Cu(II),\ pgHA}$-5](btDC) complex. The two La^{3+}[15-$MC_{Cu(II),\ pgHA}$-5]s dimers in the asymmetric unit are bridged by either a *cis*- or a *trans*-btDC (Figure 2a or 2b, respectively). A second btDC is bound to the hydrophobic face of each MC. This guest extends bridges a Cu^{2+} ring metal on the hydrophilic face of another MC in the lattice, resulting in a coordination polymer. In this structure the length of btDC prevents formation of the cylindrically shaped compartment, as the MCs in the dimer are horizontally displaced by over 8 Å. Importantly, the pgHA phenyl rings on opposite MCs do not associate through π-stacking interactions. While some van der Waals interactions between pgHA side chains are observed, the association of the side chains primarily occurs through the packing of interstitial DMF solvent molecules. Overall, this structure does not fit the criteria of a compartment (vide supra), further demonstrating how long guests can disrupt intermetallacrown interactions.

As expected, the longer hpheHA side chain renders the Ln^{3+}[15-$MC_{Cu(II),\ hpheHA}$-5] host capable of encapsulating longer guests than hosts with pheHA or pgHA side chains. The crystal structure of the Gd^{3+}[15-$MC_{Cu(II),\ hpheHA}$-5](btDC) complex reveals a 15.2 Å cylindrical compartment that encapsulates the 9.2 Å btDC guest (Figure 3). The btDC guest is bound bidentate to 8-coordinate Gd^{3+} central metals. Many π-stacking interactions are observed between ligands across the hydrophobic faces and the aromatic rings on the guest. As a whole, these structures reveal that the maximum height of the compartment is dictated by the side-chain length. Encapsulation of the 5.8 Å long terephthalate is observed with the pheHA side chain and not with the shorter pgHA. Similarly, encapsulation of the 9.2 Å long btDC is observed with the hpheHA side chain and not with pheHA or pgHA.

Interestingly, the La^{3+}[15-$MC_{Cu(II),\ hpheHA}$-5](isonicotinate) complex reveals that compartments can also be disrupted by excessively short guests. Isonicotinate is effectively encapsulated in compartments with Gd^{3+}[15-$MC_{Cu(II),\ pheHA}$- 5],

dx.doi.org/10.1021/ic202347j | *Inorg. Chem.* 2012, 51, 4527−4538

Table 1. Summary of Crystal Data and Experimental Details for All Host–Guest Complexes

	Gd^{3+}[15-$MC_{Cu(II),\ pgHA}$-5] (terephthalate)	La^{3+}[15-$MC_{Cu(II),\ pgHA}$-5](btDC)	Gd^{3+}[15-$MC_{Cu(II),\ hpheHA}$-5] (btDC)	La^{3+}[15-$MC_{Cu(II),\ hpheHA}$-5] (isonicotinate)	La^{3+}[15-$MC_{Cu(II),\ pheHA}$-5] (isonicotinate)	La^{3+}[15-$MC_{Cu(II),\ pgHA}$-5](isonicotinate)	La^{3+}[15-$MC_{Cu(II),\ pheHA}$-5] (terephthalate)	La^{3+}[15-$MC_{Cu(II),\ hpheHA}$-5] (terephthalate)	Gd^{3+}[15-$MC_{Cu(II),\ hpheHA}$-5] (terephthalate)
molecular formula	$GdCu_5C_{56}H_{87}N_{10}O_{37}$	$La_4Cu_2C_{237}H_{282}N_{50}O_{103.5}S_{12}$	$Gd_2Cu_{10}C_{154.25}H_{225}N_{28}O_{58.25}S_6$	$LaCu_5C_{63}H_{94.5}N_{13}O_{29.25}$	$La_2Cu_5C_{115}H_{148}N_{26}O_{49}$	$La_2Cu_{10}C_{110}H_{184.8}N_{25}O_{53.58}$	$La_2Cu_{10}C_{106}H_{149}N_{22}O_{54.5}$	$La_2Cu_{10}C_{130.5}H_{211.5}N_{20}O_{65.25}$	$Gd_2Cu_{10}C_{128}H_{183.5}N_{20}O_{53.75}$
mol wt [g mol^{-1}]	1967.31	7698.29	4545.88	1958.63	3591.81	3628.13	3516.69	4017.92	3812.35
cryst syst	orthorhombic	monoclinic	monoclinic	tetragonal	triclinic	orthorhombic	triclinic	monoclinic	triclinic
space group	$P2_12_12_1$	$P2_1$	$P2_1$	$P4_12_12$	P_1	$P2_12_12_1$	P_1	$P2_1$	P_1
a [Å]	14.5520(14)	15.5616(14)	16.7609(9)	16.4964(3)	15.082(5)	16.966(3)	15.1391(12)	21.897(3)	15.4739(6)
b [Å]	15.9599(15)	30.839(3)	35.759(2)	16.4964(3)	15.242 (5)	27.984(4)	15.5615(12)	16.761(2)	15.7235(6)
c [Å]	31.340(3)	30.729(3)	17.9482(10)	61.5156(18)	17.234 (8)	32.407(5)	17.1216(14)	23.454(3)	16.5063(6)
α [deg]	90	90	90	90	74.492 (4)	90	72.100(1)	90	106.389(1)
β [deg]	90	100.620(7)	107.712(1)	90	67.296 (7)	90	77.870(1)	98.896(2)	99.092(1)
γ [deg]	90	90	90	90	71.961(5)	90	66.827(1)	90	98.734(1)
vol. [$Å^3$]	7274.2(12)	14494(2)	10247.4(1.0)	16740.3(7)	3425(2)	15386(4)	3510.3(5)	8519.7(1.8)	3721.8(2)
Z	4	2	2	8	1	4	1	2	1
density, ρ [g cm^{-3}]	1.796	1.764	1.473	1.554	1.741	1.566	1.664	1.566	1.701
abs coeff, μ [mm^{-1}]	2.436	2.192	1.795	1.830	2.222	1.981	2.168	1.802	2.368
$F(000)$	3992	7764	4653	7996	1816	7410	1779	4121	1940
cryst size [mm^3]	0.15 × 0.14 × 0.14	0.11 × 0.03 × 0.01	0.36 × 0.30 × 0.18	0.21 × 0.17 × 0.03	0.25 × 0.17 × 0.09	0.28 × 0.24 × 0.20	0.38 × 0.22 × 0.03	0.40 × 0.34 × 0.09	0.31 × 0.26 × 0.22
θ range for data collection [deg]	1.30–28.38	0.74–29.08	1.14–29.59	1.75–25.81	1.63–29.71	1.74–29.58	1.83–9.64	0.88–28.38	2.08–31.48
limiting indices	$-19 < h < 19$	$-19 < h < 19$	$-23 < h < 23$	$20 < h < 2$	$-20 < h < 20$	$-23 < h < 23$	$-21 < h < 2$	$-29 < h < 29$	$-22 < h < 22$
	$-21 < k < 21$	$-38 < k < 38$	$-49 < k < 49$	$-20 < k < 20$	$-21 < k < 21$	$-38 < k < 38$	$-21 < k < 21$	$-22 < k < 22$	$-23 < k < 23$
	$-41 < l < 41$	$-38 < l < 38$	$-24 < l < 24$	$-75 < l < 74$	$-23 < l < 23$	$-44 < l < 44$	$-23 < l < 23$	$-31 < l < 31$	$-24 < l < 24$
measured reflns	258 417	252 123	409 925	314 012	37 707	708 432	173 395	287 865	156 633
independent reflns	18 148	59 688	57 566	16 062	37 707	43 117	39 247	42 596	45 283
completeness to θ	0.998	0.997	1.000	0.998	0.983	0.999	0.997	0.997	0.947
data/restraints/ parameters	18 148/12/973	59 688/446/3775	57 566/2500/2741	16 062/820/1066	37 707/4/ 1829	43 117/335/2152	39 247/682/2125	42 596/2296/2294	45 283/159/1968
goodness of on F^2	1.123	0.992	1.154	1.244	0.738	1.085	1.027	1.204	1.030
final R indices [I > 2ρ (I)]	R_1 = 0.0435, wR_2 = 0.1263	R_1 = 0.0558, $wR2$ = 0.1246	R_1 = 0.0550, wR_2 = 0.1540	R_1 = 0.0948, wR_2 = 0.2034	R_1 = 0.0571, wR_2 = 0.1758	R_1 = 0.0379, wR_2 = 0.1110	R_1 = 0.0523, wR_2 = 0.1373	R_1 = 0.0482, wR_2 = 0.1324	R_1 = 0.0364, wR_2 = 0.0924
R indices (all data)	R_1 = 0.0540, wR_2 = 0.1390	R_1 = 0.1076 wR_2 = 0.1610	R_1 = 0.0592 wR_2 = 0.1580	R_1 = 0.1051 wR_2 = 0.2075	R_1 = 0.0640, wR_2 = 0.1839	R_1 = 0.0421 wR_2 = 0.1152	R_1 = 0.0663 wR_2 = 0.1516	R_1 = 0.0518 wR_2 = 0.1364	R_1 = 0.0415 wR_2 = 0.0967
largest diff. peak and hole [e $Å^{-3}$]	1.892 and −1.595	2.750 and −1.581	2.127 and −1.3933	1.119 and −1.550	2.389 and −1.878	2.469 and −1.761	2.062 and −1.289	1.466 and −2.119	1.469 and −0.783

dx.doi.org/10.1021/ic202347j | Inorg. Chem. 2012, 51, 4527–4538

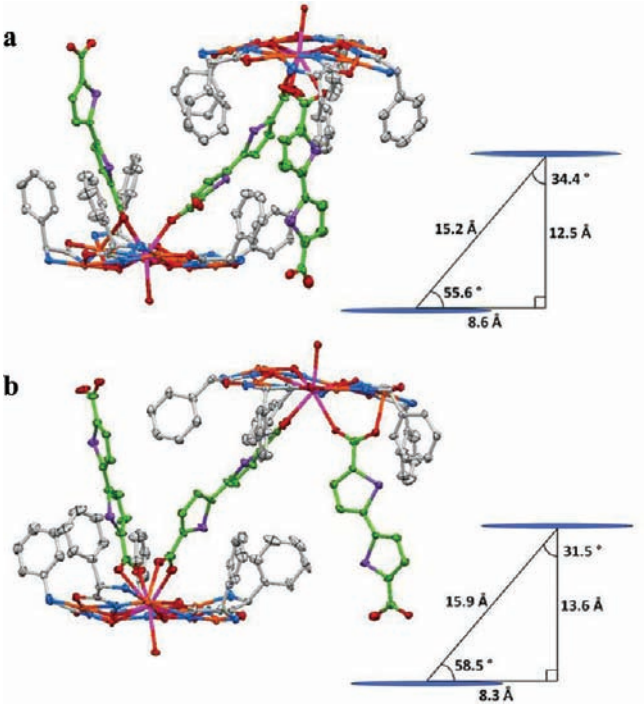

Figure 2. Thermal ellipsoid plots and compartment diagrams for $La^{3+}[15\text{-}MC_{Cu(II),\ pgHA}\text{-}5](btDC)$ showing the MC dimers bridged by (a) *cis*-btDC and (b) *trans*-btDC. Crystal structure color scheme: pink = La, orange = Cu, red = O, dark blue = N, gray = MC C, green = guest C, purple = sulfur. Solvent molecules and hydrogen atoms were removed for clarity. Thermal ellipsoids are displayed at the 50% probability level.

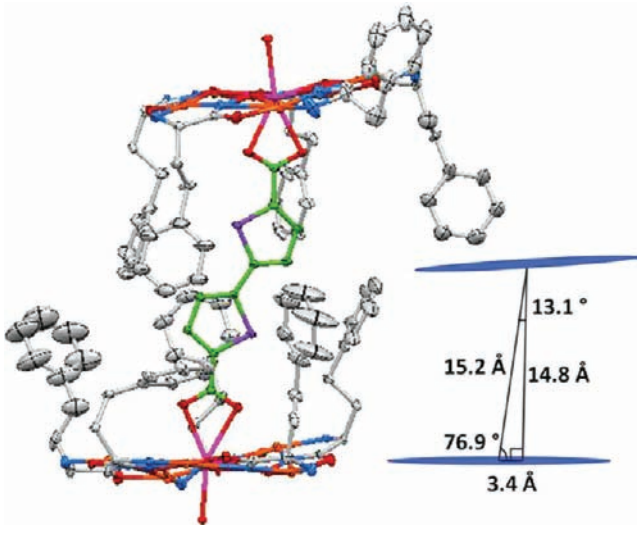

Figure 3. Thermal ellipsoid plot and compartment diagram of $Gd^{3+}[15\text{-}MC_{Cu(II),\ hpheHA}\text{-}5](btDC)$. Crystal structure color scheme: pink = Gd, orange = Cu, red = O, dark blue = N, gray = MC C, green = guest C, purple = S. Guests on the hydrophilic face, unbound counteranions, solvent molecules, and hydrogen atoms were removed for clarity. Thermal ellipsoids are displayed at the 50% probability level.

$La^{3+}[15\text{-}MC_{Cu(II),\ pheHA}\text{-}5]$, and $La^{3+}[15\text{-}MC_{Cu(II),\ pgHA}\text{-}5]$ hosts (vide infra). However, the $La^{3+}[15\text{-}MC_{Cu(II),\ hpheHA}\text{-}5]$ does not form a compartment with the 4.3 Å long isonicotinate. In the structure, two isonicotinate guests are bound in a monomeric

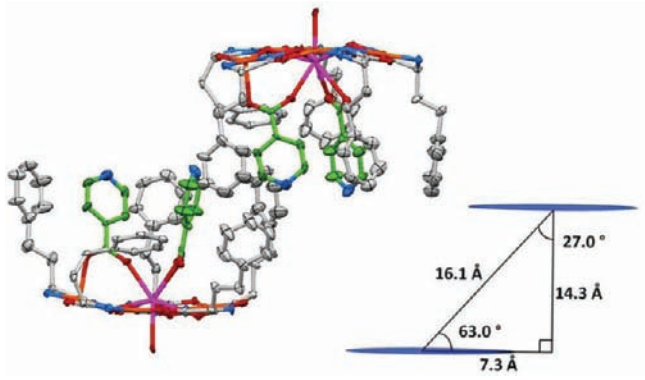

Figure 4. Thermal ellipsoid plot and compartment diagram of $La^{3+}[15\text{-}MC_{Cu(II),\ hpheHA}\text{-}5](isonicotinate)$. Crystal structure color scheme: pink = La, orange = Cu, red = O, dark blue = N, gray = MC C, green = guest C. Guests on the hydrophilic face, unbound counteranions, solvent molecules, and hydrogen atoms were removed for clarity. Thermal ellipsoids are displayed at the 50% probability level.

$La^{3+}[15\text{-}MC_{Cu(II),\ hpheHA}\text{-}5]$ hydrophobic cavity (Figure 4). Inclusion of two guests is afforded by an additional coordination site on the nine-coordinate La^{3+} central metal. The isonicotinates are bound through their carboxylates, with one bidentate to La^{III} and the other bridging the central metal and a Cu^{II} ring metal. The pyridyl nitrogens are unbound, extending out of the hydrophobic cavity and hydrogen bonding to lattice water molecules. The two monomeric MCs associate via π-stacking interactions with a 16.1 Å MC−MC distance. However, the monomers are significantly offset with a 7.3 Å horizontal displacement relative to each other. This demonstrates that though compartments can compress to accommodate short guests, the extent that they will compress is limited by the side-chain length.

As a whole, the $Ln^{3+}[15\text{-}MC_{Cu(II)}\text{-}5]$ compartment structures described heretofore and in previous work[42,48,52,56−58] reveal that the side-chain length constrains the maximum and minimum compartment height. The assembly of the compartment through nondirectional hydrophobic interactions between the flexible side chains gives the dimeric compartment a margin of a few Angstroms where it can adapt to a certain guest. However, the compartment can be readily disrupted by extremely long or short guests. These results suggest that as a guideline for designing $Ln^{3+}[15\text{-}MC_{Cu(II)}\text{-}5]$ compartment inclusion compounds the side-chain length should be complementary with the length of the guest.

Factors Influencing the Number of Encapsulated Guests. Inclusion of multiple guests is appealing from the viewpoint of multimolecular reactions in the interior of a host or the design of materials. We sought to establish the factors that promote inclusion of multiple guests in dimeric $Ln^{3+}[15\text{-}MC_{Cu(II)}\text{-}5]$ compartments. Analysis of the crystal structures of the series of $Ln^{3+}[15\text{-}MC_{Cu(II)}\text{-}5]$ host−guest complexes reveals that steric interactions with the side chain, compartment compression or elongation, and central lanthanide coordination number all influence the number of encapsulated guests.

The effect of side-chain sterics is most evident by comparing the $La^{3+}[15\text{-}MC_{Cu(II),\ pheHA}\text{-}5](isonicotinate)$ and $La^{3+}[15\text{-}MC_{Cu(II),\ pgHA}\text{-}5](isonicotinate)$ structures. Three isonicotinate guests are encapsulated in the $La^{3+}[15\text{-}MC_{Cu(II),\ pheHA}\text{-}5]$ compartment (Figure 5), while five are encapsulated in the

dx.doi.org/10.1021/ic202347j | *Inorg. Chem.* 2012, 51, 4527−4538

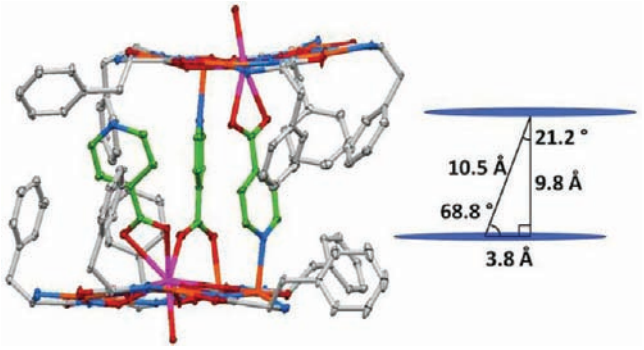

Figure 5. Thermal ellipsoid plot and compartment diagram of La^{3+}[15-$MC_{Cu(II),\ pheHA}$-5](isonicotinate). Crystal structure color scheme: pink = La, orange = Cu, red = O, dark blue = N, gray = MC C, green = guest C. Guests on the hydrophilic face, unbound counteranions, solvent molecules, and hydrogen atoms were removed for clarity. Thermal ellipsoids are displayed at the 50% probability level.

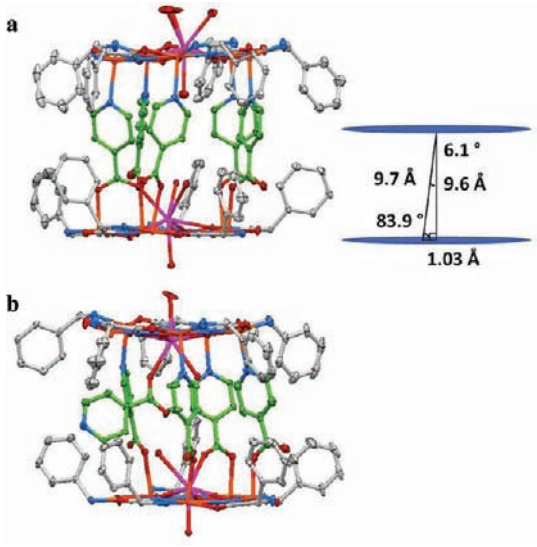

Figure 6. Thermal ellipsoid plots and compartment diagram of La^{3+}[15-$MC_{Cu(II),\ pgHA}$-5](isonicotinate). Structure is disordered between two compartment orientations, with all isonicotinates aligned (a) and one isonicotinate perpendicular (b). Color scheme: pink = La, orange = Cu, red = O, dark blue = N, gray = MC C, green = guest C. Unbound counteranions, solvent molecules, and hydrogen atoms were removed for clarity. Thermal ellipsoids are displayed at the 50% probability level.

La^{3+}[15-$MC_{Cu(II),\ pgHA}$-5] complex (Figure 6). The La^{3+}[15-$MC_{Cu(II),\ pheHA}$-5](isonicotinate) complex closely resembles the previously reported structure that had a Gd^{3+} central metal.[52] The La^{3+}[15-$MC_{Cu(II),\ pheHA}$-5] compartment has a height of 10.5 Å. Two isonicotinates are aligned antiparallel, with the pyridine coordinated to a Cu^{2+} ring metal and at least one carboxylate oxygen atom bound to a La^{3+} central metal. The third isonicotinate binds bidentate to a La^{3+} and does not span the dimer, instead extending toward the periphery of the MC.

The La^{3+}[15-$MC_{Cu(II),\ pgHA}$-5](isonicotinate) compartment is 9.7 Å in height and encapsulates 5 guests. The structure is disordered between two components with 75% and 25% occupancy (Figure 6a and 6b, respectively). In component a, the five isonicotinate guests are aligned parallel as they bridge the compartment. One carboxylate bridges a nine-coordinate La^{3+} and a ring metal, while the remaining four are bound monodentate to a ring metal. In component b, only four of the isonicotinates are parallel. The fifth is roughly perpendicular, with the pyridine group oriented to the periphery of the host.

The distinction between the inclusion of three or five guests in the La^{3+}[15-$MC_{Cu(II),\ pheHA}$-5](isonicotinate) and La^{3+}[15-$MC_{Cu(II),\ pgHA}$-5](isonicotinate) compartments suggests that the length and orientation of the phenyl side chain can influence the number of encapsulated guests. With pgHA, the phenyl side chain is rigidly extended to the periphery of the MC. Thus, there are minimal steric effects obstructing inclusion of multiple isonicotinates. In contrast, the pheHA side chains are no longer more flexible. They are observed converging on guests bound in the hydrophobic cavity. This recognition by the more flexible side chain likely introduces steric interactions which hinder the binding of additional guests. This effect of side-chain convergence limiting the guest accessibility to the host is most evident in compartment volumes measurements. Compartment volumes were estimated with Platon[68] by comparing the void space of the crystal structure with and without encapsulated guests. The solvent-accessible void space of the structure was measured with and without the encapsulated substrates in the interior of the compartment, which entails the carboxylate guests and other counterions or solvent molecules. The difference in the void spaces of the complete structure from that of the empty compartment gave the estimate for the volume of the host. These values are tabulated in Table 2 for complexes with well-defined compartments. The guest volume was measured in Discovery Studio Visualizer by rolling a 1.4 Å probe over the surface of the guest. The volume of a water molecule was set as 11.5 $Å^3$.[69] The compartment and guest volumes were used to determine the packing coefficient, defined as the percentage of the host volume filled by the guests. A previous study has reported that the optimal packing coefficient for guest inclusion is 55 ± 9%, though this is expected to be higher in assemblies with highly polar host−guest interactions.[70] Packing coefficients for select Ln^{3+}[15-MC-5] compartments are listed in Table 2. The volume of the La^{3+}[15-$MC_{Cu(II),\ pgHA}$-5](isonicotinate) compartment is 710.3 $Å^3$. The volume of the La^{3+}[15-$MC_{Cu(II),\ pheHA}$-5](isonicotinate) compartment is over 30% less at 480.3 $Å^3$. The compartment volumes reflect how longer, more flexible side chains can converge on substrates in the hydrophobic cavity and limit the number of encapsulated guests.

The inclusion of multiple guests also seems to be promoted by compartment compression. When compartments compress with a short bridging guest, the side chains must splay out toward the periphery of the MC, which widens the compartment and increases the volume of the host. The effects of compartment compression are evident when comparing the inclusion complexes of the Ln^{3+}[15-$MC_{Cu(II),\ pheHA}$-5] hosts with isonicotinate and terephthalate. As previously described, the La^{3+}[15-$MC_{Cu(II),\ pheHA}$-5](isonicotinate) compartment compresses to a mere 10.5 Å in height. This compression promotes inclusion of three guests.

In contrast, the taller Ln^{3+}[15-$MC_{Cu(II),\ pheHA}$-5]-(terephthalate) compartments are consequentially narrower, which likely explains why only one guest is encapsulated. The structure of the La^{3+}[15-$MC_{Cu(II),\ pheHA}$-5](terephthalate) complex (Figure 7) resembles the previously reported Gd^{3+} complex. The La^{3+}[15-$MC_{Cu(II),\ pheHA}$-5](terephthalate) compartment

dx.doi.org/10.1021/ic202347j | Inorg. Chem. 2012, 51, 4527−4538

Table 2. Size and Guest Inclusion Parameters for Ln^{3+}[15-MC-5] Compartments

MC	guest	V_{host} (Å^3)	V_{guest} (Å^3)	P.C. (%)	no. of guests	Ln^{3+} coord. no.[a]	compartment height (Å)
La^{3+}[15-$MC_{Cu(II),pgHA}$-5]	isonicotinate	710.3	463.8	65.3	5	9, 9, 9, 8	9.7
La^{3+}[15-$MC_{Cu(II),pheHA}$-5]	isonicotinate	480.3	306.3	68.5	3	9, 8	10.5
Gd^{3+}[15-$MC_{Cu(II),pheHA}$-5][52]	isonicotinate	392.0	257.6	65.7	3	8, 7	10.3
La^{3+}[15-$MC_{Cu(II),hpheHA}$-5][b]	isonicotinate	292.4	171.7	58.7	2	9	*c*
Gd^{3+}[15-$MC_{Cu(II),pgHA}$-5]	terephthalate	*d*	*d*	*d*	0	8	*c*
La^{3+}[15-$MC_{Cu(II),pheHA}$-5]	terephthalate	380.0	175.4	48.3	1	8, 8	12.4
Gd^{3+}[15-$MC_{Cu(II),pheHA}$-5][42]	terephthalate	375.3	217.6	58.0	1	8, 8	11.9
La^{3+}[15-$MC_{Cu(II),hpheHA}$-5]	terephthalate	526.7	325.7	61.8	2	9, 9	12.2
Gd^{3+}[15-$MC_{Cu(II),hpheHA}$-5]	terephthalate	277.5	170.6	61.5	1	8, 8	11.9
La^{3+}[15-$MC_{Cu(II),pgHA}$-5]	btDC	*d*	*d*	*d*	2[e]	9, 9, 9, 9	15.2, 15.9
La^{3+}[15-$MC_{Cu(II),pheHA}$-5][57]	btDC	*d*	*d*	*d*	2[e]	9, 9	*c*
Gd^{3+}[15-$MC_{Cu(II),hpheHA}$-5]	btDC	495.7	332.5	67.1	1	8, 8	15.2

[a]Listed for each distinct MC in the asymmetric unit. [b]Volume of the monomeric cavity is reported. [c]Structure did not contain a formal dimeric MC complex. [d]Structure did not contain a discrete, complete compartment. [e]Number of guests bound on the hydrophobic face of each MC.

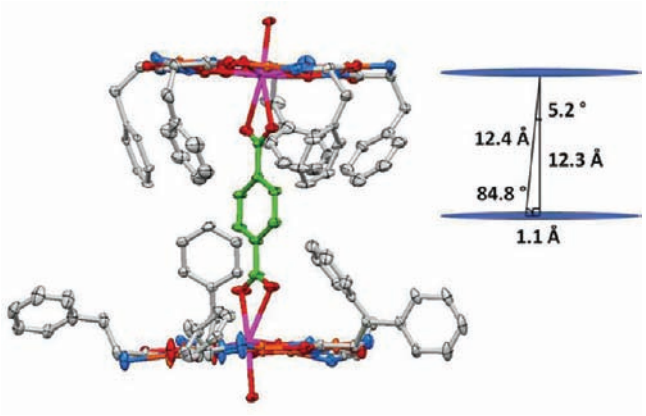

Figure 7. Thermal ellipsoid plot and compartment diagram of La^{3+}[15-$MC_{Cu(II),\ pheHA}$-5](terephthalate). Color scheme: pink = La, orange = Cu, red = O, dark blue = N, gray = MC C, green = guest C. Unbound counteranions, solvent molecules, and hydrogen atoms were removed for clarity. Thermal ellipsoids are displayed at the 50% probability level.

has a height of 12.4 Å, with one encapsulated terephthalate bridging the La^{3+} central metals. With terephthalate, the compartment is elongated, which forces the side chains toward the center in order to maintain associative interactions with the opposite MC in the dimer. The narrow compartment can only accommodate one guest. Thus, these structures demonstrate that compressed compartments can have wider interiors, which promote inclusion of multiple guests.

Differences in guest charge likely do not influence the number of encapsulated guests because MCs typically achieve charge balance with unbound anions in the lattice and by binding anions on the hydrophilic face. Though the overall +6 charged MC dimer would be expected to bind more −1 charged isonicotinates than −2 charged terephthalates, guest binding on the hydrophilic face prevents guest charge from factoring significantly in guest inclusion in the interior of the compartment. All MCs in La^{3+}[15-$MC_{Cu(II),\ pheHA}$-5]-(isonicotinate) and La^{3+}[15-$MC_{Cu(II),\ pheHA}$-5](terephthalate) have two bound carboxylates. This suggests the number of encapsulated guests in the hydrophobic compartment arises largely from the supramolecular behavior of the container and not merely electrostatic effects. It should also be noted that the soft pyridyl group prefers to bind to the Cu^{2+} ring metal, while the hard carboxylate has a higher affinity for the hard Ln^{3+} central metal. This drives isonicotinate to bind further toward the periphery of the compartment, while terephthalate has the highest affinity for the center of the compartment. The peripheral binding of isonicotinate can also factor into inclusion of multiple guests.

The effect of compartment compression is further demonstrated in the La^{3+}[15-$MC_{Cu(II),\ hpheHA}$-5](terephthalate) complex (Figure 8), which contains two terepthalate guests

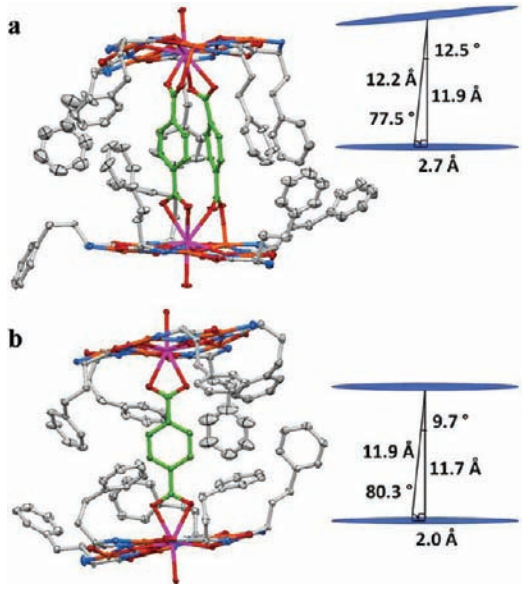

Figure 8. Thermal ellipsoid plots and compartment diagrams of (a) La^{3+}[15-$MC_{Cu(II),\ hpheHA}$-5](terephthalate) and (b) Gd^{3+}[15-$MC_{Cu(II),\ hpheHA}$-5](terephthalate). Crystal structure color scheme: pink = Gd or La, orange = Cu, red = O, dark blue = N, gray = MC C, green = guest C. Guests on the hydrophilic face, unbound counteranions, solvent molecules, and hydrogen atoms were removed for clarity. Thermal ellipsoids are displayed at the 50% probability level.

encapsulated in a 12.2 Å compartment. The terephthalates are bound with one carboxylate bidentate to the central nine-coordinate La^{3+} and the other bridging the central metal and a Cu^{2+} ring metal. The terephthalate guests engage in π-stacking interactions and a CH−O interaction with the phenyl side chains. The compartment is roughly cylindrical, with the MC

dx.doi.org/10.1021/ic202347j | Inorg. Chem. 2012, 51, 4527−4538

faces offset by 2.7 Å. The effect of compartment compression is reflected in the 526.7 Å^3 host volume. This volume is almost 150 Å^3 larger than the La^{3+}[15-MC$_{Cu(II),\ pheHA}$-5](terephthalate) compartment, which encapsulates only one terephthalate guest.

Comparison with the Ln^{3+}[15-MC$_{Cu(II),\ hpheHA}$-5]-(terephthalate) complexes with La^{3+} and Gd^{3+} central metals demonstrates that the central metal coordination number is also a factor in the number of encapsulated guests. In the Gd^{3+}[15-MC$_{Cu(II),\ hpheHA}$-5](terephthalate) structure (Figure 8b), one terephthalate guest is encapsulated in an 11.9 Å tall compartment. The terephthalate is bound bidentate at each carboxylate group to an 8-coordinate Gd^{3+} central metal. The volume of the compartment is merely 277.5 Å^3, about one-half of the La^{3+}[15-MC$_{Cu(II),\ hpheHA}$-5](terephthalate) compartment. The disparity between the number of encapsulated guests with Gd^{3+} and La^{3+} complexes is from the different coordination number on the metal ions. Similar to the structures of monomeric MC−guest complexes, the eight-coordinate Gd^{3+} preferentially accommodates one bidentate carboxylate; thus, Gd^{3+}[15-MC-5] compartments are likely to bind one dicarboxylate guest. In contrast, the nine-coordinate La^{3+} can bind one bidentate carboxylate and one carboxylate that bridges with a Cu^{2+} ring metal, leading to inclusion of two carboxylate guests.

It is worth considering why La^{3+} central metals are occasionally 8 coordinate in certain compartment complexes. Lanthanide ions are known to adopt lower coordination numbers due to steric clashes with bound substrates. It is likely that steric effects from substituents and the MC face, such as side chains converging at the MC center or bound guests, lead to lower coordination numbers. The La^{3+}[15-MC$_{Cu(II),\ pheHA}$-5]-(terephthalate) compartment is slightly stretched in order to accommodate terephthalate, which forces the side chains inward. Steric effects from this side-chain conformation cause a La^{3+} ion to be 8-coordinate. Due to the somewhat constrained volume of the compartment, guest inclusion can also reduce the central metal coordination number. For example, some of the La^{3+} central metals in the La^{3+}[15-MC$_{Cu(II),\ pheHA}$-5]-(isonicotinate), La^{3+}[15-MC$_{Cu(II),\ pgHA}$-5](isonicotinate), and La^{3+}[15-MC$_{Cu(II),\ pheHA}$-5](ferrocene dicarboxylate) compartments adopt 8-coordinate geometries due to the steric bulk of the guests. Similarly, the Gd^{3+}[15-MC$_{Cu(II),\ pheHA}$-5]-(isonicotinate) complex likely has a 7-coordinate Gd^{3+} central metal due to steric effects.

Considering these structures together reveals that the number of encapsulated guests in Ln^{3+}[15-MC-5] compartments is influenced by steric effects from the size of the side chain, steric effects from compression or elongation of the compartment, and preferred coordination number of the central lanthanide ion. Due to the flexibility of the host, the compartment volumes can vary significantly from one host−guest complex to another, making extraction of firm rules difficult. However, these results generate the guidelines that larger lanthanide central metals, compressed compartments, and the orientation of inflexible ligands to the periphery of the compartment promote the inclusion of multiple guests.

ESI-MS of Ln^{3+}[15-MC-5](guest) Complexes. There is interest in utilizing Ln^{3+}[15-MC-5] compartments in solution applications such as supramolecular catalysts or in solution-processed materials. ESI-MS is a useful technique for qualitatively assessing host−guest interactions. While it is a gas-phase technique, experimentally observed ions correspond to species that persist in solution.[71] ESI-MS spectra of the complexes between Ln^{3+}[15-MC-5]s and their dicarboxylate guests were taken to assess whether or not dimerization occurs in solution with these complexes.

Spectra were taken of the crystalline host−guest complexes dissolved in 4:1 methanol/water and injected via a syringe pump at a range of cone voltages (10−75 mV). For all host−guest complexes, monomeric 1:1 and 1:2 MC−guest species were observed, consistent with previous results. More importantly, dimeric MC−guest species were present for all host−guest complexes. These peaks typically had weaker intensity than the monomeric MC species, though they were discernible over the background noise. With isonicotinate, 2:3 MC−guest species are observed as 3+ cations. 2:2 Ln^{3+}[15-MC-5]-guest peaks are observed with terephthalate and btDC (Figure 9). These species correspond to 3+ charged MC dimers

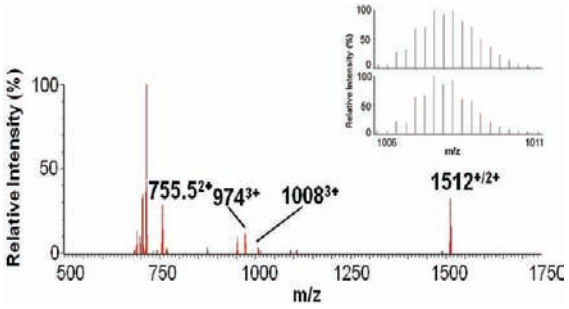

Figure 9. ESI-MS spectra of La^{3+}[15-MC$_{Cu(II),\ pheHA}$-5](terephthalate) taken in 4:1 methanol/water (v/v) injected via syringe pump. Important peaks are observed at m/z = 755.5^{2+} for La^{3+}[15-MC$_{Cu(II),\ pheHA}$-5](terephthalateH)}$^{2+}$, 973.9^{3+} for {La^{3+}[15-MC$_{Cu(II),\ pheHA}$-5]}$_2$(terephthalate)(NO$_3$)$^{3+}$, 1008.0^{3+} for {La^{3+}[15-MC$_{Cu(II),\ pheHA}$-5]}$_2$(terephthalate)(terephthalateH)$^{3+}$, and 1511.7^{+} for La^{3+}[15-MC$_{Cu(II),\ pheHA}$-5](terephthalate)$^{+}$ and {La^{3+}[15-MC$_{Cu(II),\ pheHA}$-5]}$_2$(terephthalate)$_2^{2+}$. (Inset) Isotope model of the{La^{3+}[15-MC$_{Cu(II),\ pheHA}$-5]}$_2$(terephthalate)(terephthalateH)$^{3+}$ peak at 1008.0^{3+} m/z.

with two dicarboxylates and one proton. Peaks corresponding to 3+ charged MC dimers with a mixture of dicarboxylate guests and nitrate, hydroxide, or methoxide anions were also observed. In addition, peaks corresponding to 2+ charged MC dimers with two completely deprotonated dicarboxylate guests were also observed. The 2+ charged 2:2 host−guest species have the same m/z as the 1+ charged 1:1 host−guest complex, though observation of half-integer peaks proves that the 2+ 2:2 species is present. Re-examination of the previously reported Gd^{3+}[15-MC$_{Cu(II),\ pheHA}$-5](terephthalate)[56] and Gd^{3+}[15-MC$_{Cu(II),\ pheHA}$-5](isonicotinate)[52] complexes also revealed dimeric MC complexes. ESI-MS spectra of Ln^{3+}[15-MC$_{Cu(II)}$-5]-(NO$_3$) complexes contain a 2:3 MC-nitrate species. Bridging nitrates have been observed crystallographically across the hydrophilic and hydrophobic faces of the MC.[55,58] Considering the disparate findings presented herein and from previous studies, it is evident that injection via a syringe pump, as opposed to high-performance liquid chromatography as previously utilized, was necessary to observe the dimers. This difference in conditions explains why the dimers were not originally observed.

Unfortunately ESI-MS does not provide structural information on whether the guests bridge across the hydrophobic or hydrophilic faces of the Ln^{3+}[15-MC-5] dimer. On the basis of the crystal structures, the simplest explanation is that isostructural species exist in solution. Overall, the ESI-MS

dx.doi.org/10.1021/ic202347j | Inorg. Chem. 2012, 51, 4527−4538

data supports that MC dimerization occurs in solution. Therefore, in the development of Ln^{3+}[15-MC-5] complexes for solution applications, it is appropriate to consider these species as dimers in solution with the appropriate guest.

CONCLUSIONS

Ln^{3+}[15-MC-5] compartments with pgHA, pheHA, and hpheHA ligands are a series of metalated supramolecular containers with distinct molecular recognition behavior. Differences in the size and selectivity of the compartments arise from how the length and flexibility of the phenyl side chains influence host dimerization and the degree that the side chain can converge on a guest. Systematic inclusion of bridging carboxylate guests in these hosts reveals that the compartment height is constrained by the length of the ligand side chain. Longer side chains allow formation of taller containers that encapsulate longer guests, as hpheHA ligands can form a 15.2 Å tall compartment. Considering the previously reported 7.70 Å tall Gd^{3+}[15-$MC_{Cu(II),\ tyrHA}$-5] container,[55] compartment height can be effectively doubled through straightforward modification of the ligand side chain. This work also demonstrates that up to five carboxylate guests can be encapsulated in Ln^{3+}[15-MC-5] compartments based on considerations of sterics, compartment compression, and central lanthanide coordination number.

Because Ln^{3+}[15-MC-5] compartments assemble through supramolecular interactions and recognize guests with flexible side chains, there is significant structural variability between different host−guest complexes. This variability makes the development of definitive rules for predicting these structures unfeasible at this juncture. However, the extensive and systematic structural characterization presented herein and in previous work has established some consistent trends in how the guest length, side-chain composition, and central metal influence compartment size and guest selectivity. We consider these trends as a theoretical framework one could use to predict the structure of an inclusion complex with Ln^{3+}[15-MC-5] compartments.

In the field of molecular encapsulation, there is a trend toward relying on rigid hosts with well-defined, permanent cavities to control host size and selectivity. However, these results demonstrate that flexible hosts can generate containers of comparable size and guest-recognition behavior to benchmark rigid systems, albeit in the solid state, while still following clear trends that allow for prediction and design. The ESI-MS data demonstrates that these flexible hosts persist in solution to some degree as well. The theoretical framework for considering factors that influence compartment size and selectivity of Ln^{3+}[15-MC-5] compartments established through previous studies and this work will guide future investigations of the hosts as reaction vessels and building blocks for porous solids and in the design of nonlinear optical materials.

ASSOCIATED CONTENT

Supporting Information

Crystallographic tables, crystallographic information files (CIF), discussion of the MC and ligand syntheses. This material is available free of charge via the Internet at http://pubs.acs.org.

AUTHOR INFORMATION

Corresponding Author

*E-mail: vlpec@umich.edu.

ACKNOWLEDGMENTS

We thank the National Science Foundation (CHE-0717098 and CHE-1057331) for funding. Crystallographic data for La^{3+}[15-$MC_{Cu(II),\ pgHA}$-5](btDC) were collected through the SCrALS (Service Crystallography at Advanced Light Source) program at the Small-Crystal Crystallography Beamline 11.3.1 at the Advanced Light Source (ALS), Lawrence Berkeley National Laboratory. The ALS is supported by the U.S. Department of Energy, Office of Energy Sciences Materials Sciences Division, under contract DE-AC02-05CH11231.

REFERENCES

(1) Yoshizawa, M.; Klosterman, J. K.; Fujita, M. *Angew. Chem., Int. Ed.* **2009**, *48*, 3418.
(2) Pluth, M. D.; Bergman, R. G.; Raymond, K. N. *Acc. Chem. Res.* **2009**, *42*, 1650.
(3) Hof, F.; Craig, S. L.; Nuckolls, C.; Rebek, J. J. *Angew. Chem., Int. Ed.* **2002**, *41*, 1488.
(4) Liu, S.; Gan, H.; Hermann, A. T.; Rick, S. W.; Gibb, B. C. *Nat. Chem.* **2010**, *2*, 847.
(5) Zhao, Y.-L.; Li, Z.; Kabehie, S.; Botros, Y. Y.; Stoddart, J. F.; Zink, J. I. *J. Am. Chem. Soc.* **2010**, *132*, 13016.
(6) Ono, K.; Yoshizawa, M.; Akita, M.; Kato, T.; Tsunobuchi, Y.; Ohkoshi, S.; Fujita, M. *J. Am. Chem. Soc.* **2009**, *131*, 2782.
(7) Tiefenbacher, K.; Dube, H.; Ajami, D.; J. Rebek, J. *Chem. Commun.* **2011**, *47*, 7341.
(8) Yebeutchou, R. M.; Tancini, F.; Demitri, N.; Geremia, S.; Mendichi, R.; Dalcanale, E. *Angew. Chem., Int. Ed.* **2008**, *47*, 4504.
(9) Berryman, O. B.; Sather, A. C.; Lledó, A.; Rebek, J. *Angew. Chem., Int. Ed.* **2011**, *50*, 9400.
(10) Atwood, J. L.; Koutsantonis, G. A.; Raston, C. L. *Nature* **1994**, *368*, 229.
(11) Kersting, B.; Lehman, U. *Adv. Inorg. Chem.* **2009**, *61*, 407.
(12) Ballester, P. *Chem. Soc. Rev.* **2010**, *39*, 3810.
(13) Schmidtchen, F. P. *Chem. Soc. Rev.* **2010**, *39*, 3916.
(14) Boisocchi, M.; Bonizzoni, M.; Fabbrizzi, L.; Piovani, G.; Taglietti, A. *Angew. Chem., Int. Ed.* **2004**, *43*, 3847.
(15) Frischmann, P. D.; Facey, G. A.; Ghi, P. Y.; Gallant, A. J.; Bryce, D. L.; Lelj, F.; MacLachlan, M. J. *J. Am. Chem. Soc.* **2010**, *132*, 3893.
(16) O'Neil, E. J.; Smith, B. D. *Coord. Chem. Rev.* **2006**, *250*, 3068.
(17) Damsyik, A.; Lincoln, S. F.; Wainwright, K. P. *Inorg. Chem.* **2006**, *45*, 9834.
(18) Sigouin, O.; Garon, C. N.; Delaunais, G.; Yin, X.; Woo, T. K.; Decken, A.; Fontaine, F.-G. *Angew. Chem., Int. Ed.* **2007**, *46*, 4979.
(19) Lindsay, V. N. G.; Lin, W.; Charette, A. B. *J. Am. Chem. Soc.* **2009**, *131*, 16383.
(20) Jeunesse, C.; Armspach, D.; Matt, D. *Chem. Commun.* **2005**, 5603.
(21) Zelder, F.; Salvio, R.; J. Rebek, J. *Chem. Commun.* **2006**, 1280.
(22) Richeter, S.; J. Rebek, J. *J. Am. Chem. Soc.* **2004**, *126*, 16280.
(23) Zelder, F.; J. Rebek, J. *Chem. Commun.* **2006**, 753.
(24) Lozan, V.; Buchholz, A.; Plass, W.; Kersting, B. *Chem.—Eur. J.* **2007**, *13*, 7305.
(25) Steinfield, G.; Lozan, V.; Kersting, B. *Angew. Chem., Int. Ed.* **2003**, *42*, 2261.
(26) Käss, S.; Gregor, T.; Kersting, B. *Angew. Chem., Int. Ed.* **2005**, *45*, 101.
(27) Klingele, J.; Klingele, M. H.; Baars, O.; Lozan, V.; Buchholz, A.; Leibeling, G.; Plass, W.; Meyer, F.; Kersting, B. *Eur. J. Inorg. Chem.* **2007**, *2007*, 5277.
(28) Mezei, G.; Zaleski, C. M.; Pecoraro, V. L. *Chem. Rev.* **2007**, *107*, 4933.
(29) Pecoraro, V. L.; Stemmler, A. J.; Gibney, B. R.; Bodwin, J. J.; Wang, H.; Kampf, J. W.; Barwinski, A. In *Progress in Inorganic Chemistry*; Karlin, K. D., Ed.; John Wiley and Sons, Inc.: New York, 1997; Vol. *45*, p 83.
(30) Pecoraro, V. L. *Inorg. Chim. Acta* **1989**, *155*, 171.

(31) Lah, M. S.; Kirk, M. L.; Hatfield, W.; Pecoraro, V. L. *J. Chem. Soc., Chem. Commun.* **1989**, 1606.
(32) Lah, M. S.; Pecoraro, V. L. *J. Am. Chem. Soc.* **1989**, *111*, 7258.
(33) Gibney, B. R.; Kessissoglou, D. P.; Kampf, J. W.; Pecoraro, V. L. *Inorg. Chem.* **1994**, *33*, 4840.
(34) Kurzak, B.; Farkas, E.; Glowiak, T.; Kozlowski, H. *J. Chem. Soc., Dalton Trans.* **1991**, 163.
(35) Kessissoglou, D. P.; Kampf, J. W.; Pecoraro, V. L. *Polyhedron* **1994**, *13*, 1379.
(36) Stemmler, A. J.; Kampf, J. W.; Pecoraro, V. L. *Angew. Chem., Int. Ed. Engl.* **1996**, *35*, 2841.
(37) Stemmler, A. J.; Barwinski, A.; Baldwin, M. J.; Young, V.; Pecoraro, V. L. *J. Am. Chem. Soc.* **1996**, *118*, 11962.
(38) Lehaire, M.-L.; Scopelliti, R.; Severin, K. *Chem. Commun.* **2002**, 2766.
(39) Pavlishchuk, A. V.; Kolotilov, S. V.; Zeller, M.; Thompson, L. K.; Fritsky, I. O.; Addison, A. W.; Hunter, A. D. *Eur. J. Inorg. Chem.* **2010**, 4851.
(40) Dendrinou-Samara, C.; Alevizopoulou, L.; Iordanidis, L.; Samaras, E.; Kessissoglou, D. P. *J. Inorg. Biochem.* **2002**, *89*, 89.
(41) Metallacrown nomenclature utilized in this manuscript is based on the following scheme: M[ring size-MCM′, L-ring oxygens](X), where M is the central metal and its oxidation state, M′ is the ring metal, L is the α-amino hydroxamic acid ligand on the MC, and X is the bound carboxylate guest.
(42) Cutland, A. D.; Halfen, J. A.; Kampf, J. W.; Pecoraro, V. L. *J. Am. Chem. Soc.* **2001**, *123*, 6211.
(43) Stemmler, A. J.; Kampf, J. W.; Kirk, M. L.; Atasi, B. H.; Pecoraro, V. L. *Inorg. Chem.* **1999**, *38*, 2807.
(44) Dallavalle, F.; Remelli, M.; Sansone, F.; Bacco, D.; Tegoni, M. *Inorg. Chem.* **2010**, *49*, 1761.
(45) Bacco, D.; Bertolasi, V.; Dallavalle, F.; Galliera, L.; Marchetti, N.; Marchio, L.; Remelli, M.; Tegoni, M. *Dalton Trans.* **2011**, *40*, 2491.
(46) Lim, C.-S.; Kampf, J. W.; Pecoraro, V. L. *Inorg. Chem.* **2009**, *48*, 5224.
(47) Tegoni, M.; Tropiano, M.; Marchio, L. *Dalton Trans.* **2009**, 6705.
(48) Jankolovits, J.; Kampf, J. W.; Maldonado, S.; Pecoraro, V. L. *Chem.—Eur. J.* **2010**, *16*, 6786.
(49) Lim, C.-S.; Jankolovits, J.; Zhao, P.; Kampf, J. W.; Pecoraro, V. L. *Inorg. Chem.* **2011**, *50*, 4832.
(50) Cutland-Van Noord, A. C.; Kampf, J. W.; Pecoraro, V. L. *Angew. Chem., Int. Ed.* **2002**, *41*, 4667.
(51) Lim, C. S.; Jankolovits, J.; Kampf, J. W.; Pecoraro, V. L. *Chem. Asian J.* **2010**, *5*, 46.
(52) Mezei, G.; Kampf, J. W.; Pan, S.; Poeppelmeier, K. R.; Watkins, B.; Pecoraro, V. L. *Chem. Commun.* **2007**, *11*, 1148.
(53) Pecoraro, V. L.; Bodwin, J. J.; Cutland, A. D. *J. Solid State Chem.* **2000**, *152*, 68.
(54) Zaleski, C. M.; Depperman, E. C.; Kampf, J. W.; Kirk, M. L.; Pecoraro, V. L. *Inorg. Chem.* **2006**, *45*, 10022.
(55) Cutland, A. D.; Malkani, R. G.; Kampf, J. W.; Pecoraro, V. L. *Angew. Chem., Int. Ed.* **2000**, *39*, 2689.
(56) Lim, C.-S.; Noord, A. D. C.-V.; Kampf, J. W.; Pecoraro, V. L. *Eur. J. Inorg. Chem.* **2007**, 1347.
(57) Jankolovits, J.; Lim, C.-S.; Kampf, J. W.; Pecoraro, V. L. *Z. Naturforsch.* **2010**, *65b*, 263.
(58) Zaleski, C. M.; Lim, C.-S.; Cutland-Van Noord, A. D.; Kampf, J. W.; Pecoraro, V. L. *Inorg. Chem.* **2011**, *50*, 7707.
(59) Wynberg, H.; Bantjes, A. *J. Am. Chem. Soc.* **2002**, *82*, 1447.
(60) Tegoni, M.; Furlotti, M.; Tropiano, M.; Lim, C.-S.; Pecoraro, V. L. *Inorg. Chem.* **2010**, *49*, 5190.
(61) *SAINT Plus, v. 7.60A*; Bruker Analytical X-ray: Madison, WI, 2008.
(62) Sheldrick, G. M. *Sadabs, Program for Empirical Absorbtion Correction of Area Detector Data, v 2008/1*; University of Göttingen: Göttingen, Germany, 2008.
(63) Sheldrick, G. M. *Acta Crystallogr.* **2008**, *A64*, 112.
(64) Sheldrick, G. M. *CELL_NOW v. 2008/2, Program for Indexing Twins and Other Problem Crystals*; University of Göttingen: Göttingen, Germany, 2008.
(65) Sheldrick, G. M. *TWINABS v. 2008/2, Program for Empirical Absorption Correction of Area Detector Data*; University of Göttingen: Göttingen, Germany, 2008.
(66) Inokuma, Y.; Kawano, M.; Fujita, M. *Nat. Chem.* **2011**, *3*, 349.
(67) The centroid of the oxygen-mean plane, meaning the five oxygen atoms in the MC ring, was calculated in Mercury 2.2. Previous work referenced compartment dimensions to the central lanthanides. Conversion between the two scales is complicated by the variable positioning of the central metal in different structures. For previously reported structures discussed in this manuscript, distances are also referenced to the centroids of the oxygen-mean plane.
(68) Spek, A. L. *J. Appl. Crystallogr.* **2003**, *36*, 7.
(69) Gerstein, M.; Chothia, C. *Proc. Nat. Acad. Sci* **1996**, *93*, 10167.
(70) Mecozzi, S.; J. Rebek, J. *Chem.—Eur. J.* **1998**, *4*, 1016.
(71) Schalley, C. A.; Rivera, J. M.; Martin, T.; Santamaria, J.; Siuzdak, G.; Rebek, J. *J. Org. Chem.* **1999**, 1325.